In Situ Transmission Electron Microscopy of Ion Irradiated Fe-Pt Alloy Thin Films

G. B. Thompson – The University of Alabama
N. W. Morgan – Argonne National Laboratory, Illinois
R. C. Birtcher – The University of Alabama

Citation of published version:

Morgan, N., Birtcher, R., Thompson, G. (2006): In Situ Transmission Electron Microscopy of Ion Irradiated Fe-Pt Alloy Thin Films. *Journal of Applied Physics*, 100(12). DOI: https://doi.org/10.1063/1.2364390

In situ transmission electron microscopy of ion irradiated Fe–Pt alloy thin films

N. W. Morgan
Department of Metallurgical and Materials Engineering, University of Alabama, P.O. Box 870202, Tuscaloosa, Alabama 35487-0202

R. C. Birtcher
Materials Science Division, Argonne National Laboratory, Building 212, 9700 South Cass Avenue, Argonne, Illinois 60439-4838

G. B. Thompson[a)]
Department of Metallurgical and Materials Engineering, University of Alabama, P.O. Box 870202, Tuscaloosa, Alabama 35487-0202

(Received 10 February 2006; accepted 19 August 2006; published online 21 December 2006)

We report the microstructural evolution during irradiation of FePt and FePt 25 at. % thin films sputter deposited onto electron transparent silicon monoxide substrates. The films were studied *in situ* for 500 keV Kr^+ irradiation up to a fluence of 10^{15} ions/cm^2 or 4 displacements/atom (dpa). Upon irradiation to approximately 1 dpa, the initial disconnected granular morphology became continuous. In particular, for FePt, accelerated grain growth was observed once the continuous morphology was achieved during ambient temperature irradiation. No atomistic (chemical) ordering from the as-deposited $A1$ phase into either the $L1_0$ FePt or $L1_2$ Fe_3Pt phases was observed during ambient temperature irradiation. After irradiation, the specimens were then *in situ* annealed. The intermetallic ordering temperature, compared to that of an unirradiated film, was lowered by $\approx$200 °C for FePt 25 at. %. No decrease in the ordering temperature was observed for irradiated FePt. The rate of FePt grain growth during annealing was very similar for both irradiated and unirradiated films over the 25–650 °C temperature range investigated. © *2006 American Institute of Physics*. [DOI: 10.1063/1.2364390]

I. INTRODUCTION

The binary Fe–Pt system has received considerable attention for a variety of magnetic related applications. The $L1_2$ phases of Fe_3Pt and $FePt_3$ have been studied for uses in exchange spring magnets, giant magnetoresistive (GMR) spin valve sensors, and shape memory technologies.[1–4] The high magnetocrystalline anisotropy $L1_0$ FePt phase has received considerable attention for use as a thermally stable, ultrahigh areal storage density media.[5–9] Nominally, when Fe–Pt compositions are sputter deposited, the high temperature solid-solution face-centered-cubic (fcc) phase ($A1$) is adopted.[9] A post-deposition annealing will phase transform the system from a metastable disordered ($A1$) phase to stable ordered ($L1_2$ or $L1_0$) phase. The annealing temperature for this transformation is typically near 500 °C, which is approximately one-half the bulk ordering temperature. However, annealing at these temperatures promotes accelerated grain coarsening and the loss of a narrow grain size distribution.[10] This is of particular concern for the use of FePt as small grain media. Recent experimental and modeling reports for FePt have suggested that a size effect exists where $L1_0$ ordering below $\approx$3.5 nm may not be possible.[11–14] From Monte Carlo simulations, Chepulskii *et al.*[13] have suggested that the size effect in ordering is kinetically limited, requiring a critical concentration of defects to promote the necessary diffusional ordering processes.

Ion irradiation has often been associated with atomistic disordering reactions but could provide critical concentration of point defects and/or appropriate lattice distortions that could facilitate ordering at lower annealing temperatures. Few studies have reported irradiation and ordering in FePt and FePd thin films.[15–17] In these reports, the films were *in situ* annealed at temperatures of $\approx$300 °C while simultaneously being irradiated with He^+ at energies of 30–130 keV. In a similar study, the He^+ ion beam current was high enough to directly heat the FePt film during irradiation.[18] At these moderately lower temperatures, chemical ordering from the $A1$ to the $L1_0$ phase was achieved. The low atomic mass of He displaces the Fe and/or Pt or Pd atoms by no more than one to three atomic distances requiring individual vacancy exchange to promote ordering.[16] There has been little to no investigation on how heavier ion irradiation could alter this particular phase transformation or its effects on the microstructure. The application of a heavier ion would generate larger cascade stages and a larger defect population which could result in significant differences in the phase transformation.

In this paper, we report the effects of 500 keV Kr^+ irradiation for two ordering compositions of an Fe–Pt alloy thin film: FePt and FePt 25 at. %. The FePt 25 at. % film experiences a bulk disorder-to-order transformation $<$500 °C than FePt. We have used *in situ* transmission electron microscopy (TEM) analysis to chronicle the ordering transformation and microstructure evolution as a function of irradiation dosage

[a)]Electronic mail: gthompson@coe.eng.ua.edu

and *in situ* annealing. This provides for a fundamental investigation of the effects of heavier ions on the order and microstructure stability for Fe–Pt alloys irradiated with heavier ions.

II. EXPERIMENT

The Fe–Pt alloy films were co-sputter-deposited from individual 99.95% pure Fe and Pt targets in an AJA ATC-1500 stainless-steel chamber. The base pressure prior to sputtering was $<1\times10^{-7}$ Torr whereupon ultrahigh purity Ar was flowed up to 5 mTorr for sputtering. The films were grown at thicknesses between 25 and 50 nm on Cu TEM grids, purchased from Ted Pella, Inc., that supported a thin electron transparent silicon monoxide substrate surface. The Formvar film on the grid was dissolved prior to depositing the Fe–Pt film. The nominal stoichiometry of each film was calculated from deposition rates and verified by energy dispersive spectroscopy (EDS) using a Hitachi S-4700 II high resolution scanning electron microscope (SEM) operated at 20 keV.

The *in situ* ion irradiations were performed using a modified Hitachi H-9000 intermediate voltage electron microscope (IVEM) at Argonne National Laboratory. The IVEM is a unique 300 keV LaB_6 filament microscope that has an ion accelerator beam line directly connected into the electron column. This allows for *in situ* TEM observations during ion irradiation. Specimens were tilted 15° with respect to the vertical axis of the TEM so that both the ion beam incident angle and the viewing screen were 15° with respect to the normal of the film. For this study, we used Kr^+ at 500 keV up to fluences of 10^{15} ions/cm^2 with *in situ* specimen annealing up to 650 °C. At these film thicknesses and irradiated energy, the vast majority of ions (>90%) are transmitted through the film and are not implanted. Collectively, the *in situ* capability allows real-time investigations of the effects of irradiation and subsequent temperature anneals on ordering and microstructure evolution.

The mean grain size and size distributions of the films were determined using IMAGEJ® analysis software.[19] Bright field images were processed with a binary threshold procedure that maximizes contrast by making every pixel either white or black. Based on the location and count of black pixels, grain boundaries were outlined and the area of each grain was computed. Assuming circular grains, the average grain size was calculated. The assumption of circular grains is reasonable based on the images reported in Figs. 1–3. Dosage displacements per atom (dpa) were calculated using stopping and range of ions in matter (SRIM) for 50 ,000 total ions and an Fe–Pt lattice binding energy of 3 eV. The camera length constant for the TEM measured lattice parameters was done by comparing the $d_{\{111\}}$ radial ring measurement from the TEM diffraction pattern to the equivalent $d_{\{111\}}$ lattice spacing value determined by x-ray diffraction for the as-deposited films. The x-ray diffraction (XRD) specimens were simultaneously deposited along with the TEM foils on a similar substrate surface. XRD was performed on a Philips X'Pert diffractometer using Cu $K\alpha$ radiation. Our calibrated camera length was in agreement with the camera length value given by the microscope's manufacturer. Based on the radial distance of the TEM diffracted rings, the indexed lattice planes and lattice parameters were determined for all irradiated films' diffraction patterns.

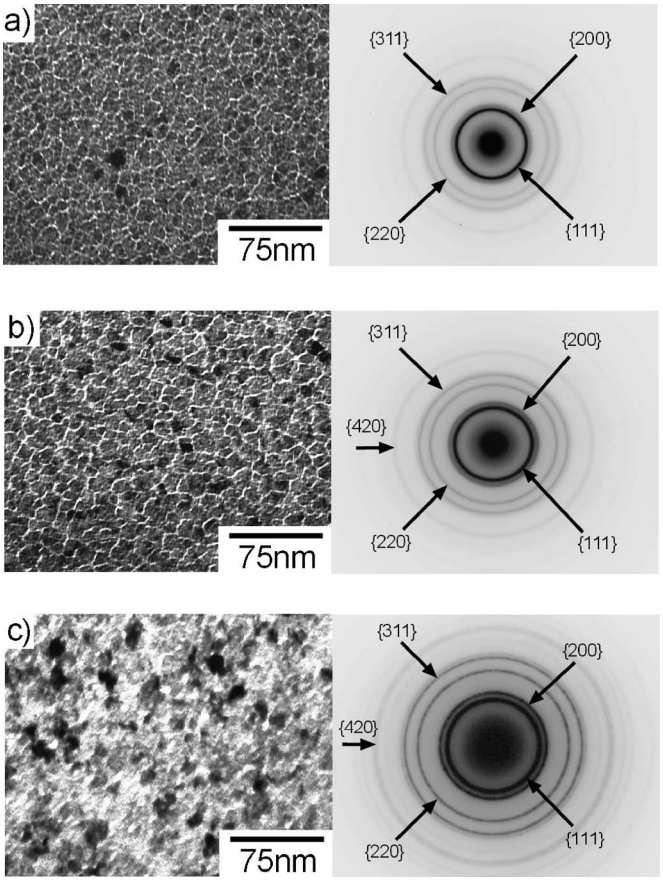

FIG. 1. (a) Bright field (BF) image and diffraction pattern (DP) of the as-prepared 25 nm thick FePt film. The pattern was indexed as the *A*1 phase. (b) BF image and DP of the 25 nm thick FePt film irradiated to 5×10^{13} ions/cm^2 (0.2 dpa). (c) BF image and DP of the 25 nm thick FePt film irradiated to 1×10^{15} ions/cm^2 (4.0 dpa). The previously disconnected nature of the grains is absent and replaced with a continuous granular microstructure.

III. RESULTS

A. FePt films

The as-deposited 25 nm FePt films were in a solid-solution face-centered-cubic (*A*1) phase with a lattice parameter of 0.383 ± 0.012 nm and a mean grain size of 8.5 ± 0.3 nm [Fig. 1(a)]. The film exhibited a discontinuous granular morphology. Irradiation fluences up to 1×10^{13} ions/cm^2 (or a dosage of 0.04 dpa) produced little to no obvious change in the microstructure. Fluences beyond 10^{13} ions/cm^2 resulted in a slight sharpening in the diffraction pattern. No atomistic (chemical) ordering superlattice reflections associated with an ordered intermetallic phase was observed. The irradiation was stopped at 1×10^{15} ions/cm^2 (or a dosage of 4.0 dpa). At the highest fluence, the initial disconnected granular morphology had evolved into a continuous granular microstructure [Fig. 1(c)].

After a dosage of 4.0 dpa, *in situ* annealing from ambient temperature up to 650 °C was performed in 50 °C steps

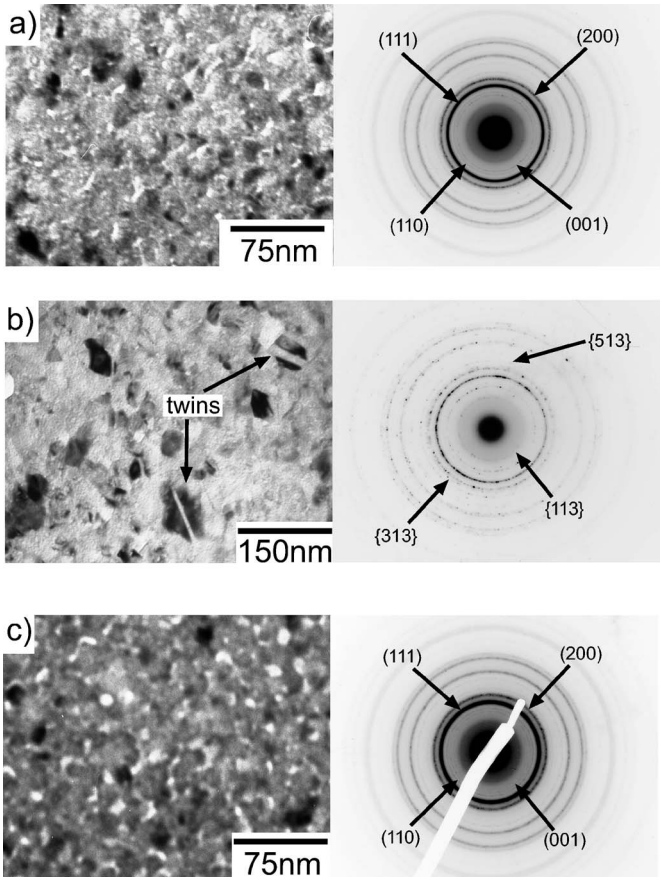

FIG. 2. (a) BF image and DP of the 25 nm thick FePt film irradiated to 4.0 dpa and annealed at 550 °C. The diffraction pattern shows the presence of two inner rings, indexed as the superlattice reflections of the $L1_0$ phase. (b) BF image and DP of the 25 nm thick FePt film irradiated to 4.0 dpa and annealed at 650 °C. Grain growth is evident in the bright field as well as many twin structures. Iron oxide reflections shown in the DP were also indexed on the diffraction pattern indicating a film-substrate interaction. (c) BF image and DP of the 25 nm thick unirradiated FePt film annealed at 550 °C.

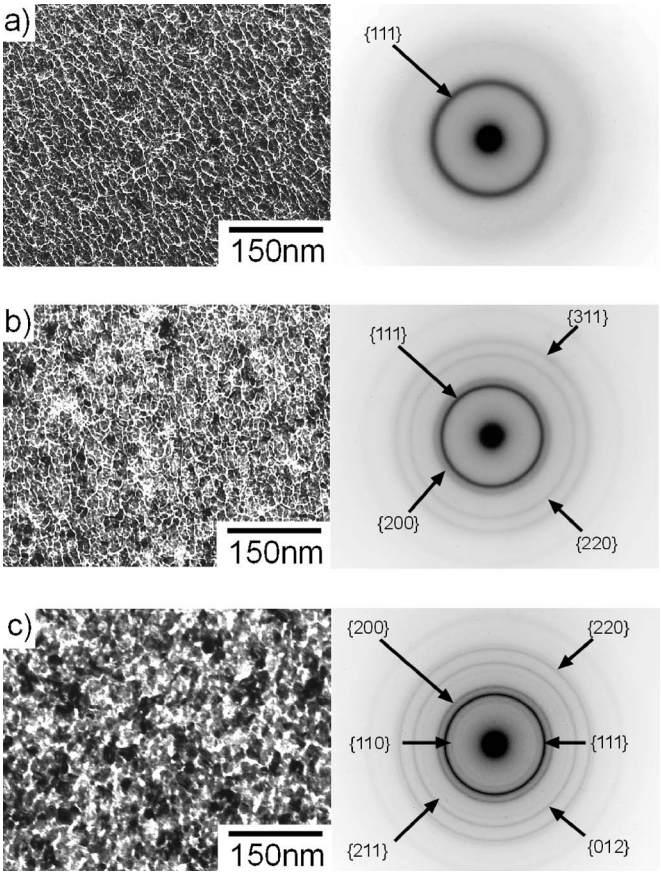

FIG. 3. (a) BF image and DP of the as-prepared 50 nm FePt 25 at. % film. A strong {111} texture is evident in the DP. The pattern was indexed as the $A1$ phase. (b) BF image and DP of the 50 nm FePt 25 at. % sample irradiated to 1×10^{13} Kr^+ ions/cm^2 (0.035 dpa). Note the addition of new (hkl) reflections along with the {111} reflection. (c) The BF image and DP of the 50 nm FePt 25 at. % film irradiated to a total of 6.25×10^{14} Kr^+ ions/cm^2 (2.2 dpa) and annealed at 300 °C. The diffraction pattern was indexed to the $L1_2$ phase.

with hold times of 10 min for each temperature step. Images and diffraction patterns were recorded at the end of each temperature-time interval. The onset of ordering, as indicated by the presence of ordered superlattice reflections (001) and (110), is observed at 550 °C [Fig. 2(a)]. The diffraction pattern in Fig. 2(a) of the 550 °C annealed FePt film was consistently indexed to a $L1_0$ phase with lattice parameters $a=0.389\pm0.012$ nm and $c=0.364\pm0.011$ nm. As the temperature was increased further, rapid grain growth and the presence of twinning was observed [Fig. 2(b)]. At 650 °C, additional $\{hkl\}$ reflections in the pattern were indexed to the γ-Fe_2O_3 phase. This suggests a substrate-film reaction at elevated temperatures and the experiment ceased. For a controlled comparison, an unirradiated FePt film was annealed at similar times and temperatures [Fig. 2(c)]. The onset of ordering was observed at 500 °C with $L1_0$ lattice parameters $a=0.384\pm0.012$ nm and $c=0.377\pm0.011$ nm. After ordering in the unirradiated film, rapid grain coarsening occurred, which is consistent with previous observations in the literature.[20] At the ordering temperature, the unirradiated film's initial disconnected granular morphology exhibited the onset of continuous film coverage over the substrate.

B. FePt 25 at. % thin films

The as-deposited 50 nm thick FePt 25 at. % films were also indexed as an $A1$ phase with a lattice parameter of $a=0.376\pm0.011$ nm. As evident in Fig. 3(a), a strong {111} ring is present. The as-deposited mean grain size was 9.0 ± 0.3 nm, slightly larger than FePt because of its larger film thickness. After 1×10^{13} ions/cm^2 (0.035 dpa), additional $A1$ $\{hkl\}$ reflections are present in the pattern, as seen in Fig. 3(b), with a corresponding increase in the diffraction contrast in the bright field image. The change in diffraction contrast with respect to the incident electron beam continued up to 1.25×10^{14} ions/cm^2 (or 0.4 dpa). Further irradiation produced no significant change in morphology. Atomistic ordering into $L1_2$ or any other phase was not observed at any of the fluences for ambient temperature irradiation. Similar to FePt, at the highest dosages, the initial disconnected granular film morphology had evolved into a continuous film.

After a 2.2 dpa dosage, the FePt 25 at. % film was annealed. At 300 °C, the presence of the $L1_2$ ordered superlattice reflection {110} was indexed with a lattice parameter $a=0.381\pm0.011$ nm. As the temperature was increased beyond this temperature, grain growth commenced [Fig. 3(c)].

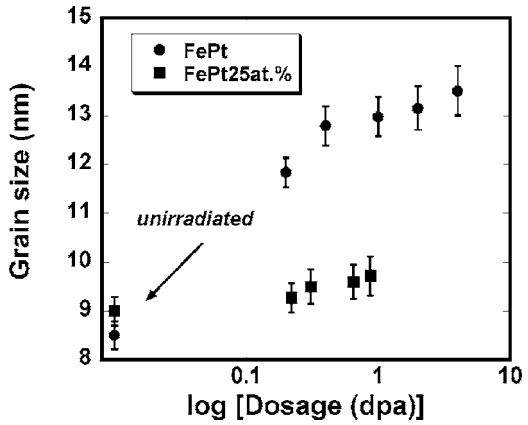

FIG. 4. Plot of grain size vs dosage for FePt and FePt 25 at. %.

At 600 °C, iron oxide reflections were present, suggesting a film-substrate interaction at elevated temperatures, and the experiment ceased. For a controlled comparison, an unirradiated FePt 25 at. % film was annealed under similar conditions. The onset of Fe_3Pt ordering occurred at ≈500 °C with a lattice parameter of 0.378±0.011 nm. Only at the ordering temperature did the disconnected granular film evolve to a continuous film coverage for the unirradiated film.

IV. DISCUSSION

As seen in the bright field images of Figs. 1 and 3, the ion irradiation above ≈0.04 dpa caused a significant change in the microstructure for each Fe–Pt composition. The films evolved from a disconnected to a continuous granular film morphology. Grain growth under ion irradiation has been reported by numerous authors.[21–24] Heavy ion irradiated grain growth is a result of either the enhancement of the grain boundary mobility by irradiation or the diffusion that can occur within a cascade volume during a thermal spike.[25] In particular, this thermal spike can induce local melting in a region of a few nanometers and resolidification after several picoseconds.[26,27] The time scale for chemical ordering in FePt is suspected to be on the order of tens of milliseconds.[28] The picosecond lifetime of an irradiation induced thermal spike does not provide sufficient time for atomistic ordering; moreover, the rapid resolidification would quench in the disordered high temperature phase. Consequently, the high temperature $A1$ phase remains after irradiation for these films.

As can be seen for Fig. 4, the dramatic rise in FePt grain growth with irradiation dosage tapers off when the grains approach 13 nm. Voegeli *et al.*[29] and Mayr and Averback[22] have shown that grain boundary migration is reduced or eliminated when the grains are larger than the thermal spike size. The experimental results of this paper suggest that the effective thermal spike has a critical in-plane grain size near 13 nm for the $A1$ phase of FePt. Interestingly, the $A1$ phase of the FePt 25 at. % film showed minimal grain growth under similar dosages. This difference could be a result of either the slightly larger layer thickness of FePt 25 at. % and/or differences in the Pt content.

The grain growth exponent n has been found using a modified grain growth equation for irradiation[24] given as

$$d^n - d_o^n = K\phi, \tag{1}$$

where d is the average grain diameter, d_o is the average initial grain size, K is a grain boundary mobility constant and ϕ is the ion dose. By a least-squares fit of the data in Fig. 4 and using Eq. (1), the grain growth exponents n for FePt and FePt 25 at. % were found to be 3.2±0.6 and 2.0±0.04, respectively. An n factor of 2 is considered a normal grain growth. Karpe *et al.*[21] have shown that Fe and Fe-rich alloys irradiated with heavy ions have n values near 2. Takahashi and Hono[20] have reported that abnormal grain growth is dominated in FePt. Our n values are consistent with these results. Abnormal grain growth can be caused by anisotropy in the grain boundary energy and mobility. In a recent Monte Carlo simulation by Yang *et al.*,[14] the total surface energy in an $A1$ phase of FePt was lowered when Pt segregated to the surface. Since the FePt and FePt 25 at. % films adopted the same $A1$ phase with relatively the same initial in-plane grain size, the grain growth anisotropy difference, noted in n and seen in Fig. 4, may be a result of the increase Pt content at the free surface (grain boundaries). This is the subject of future work.

During the ion-induced grain growth, the microstructure exhibited an increase in diffraction contrast, as seen in Figs. 1 and 3. This was confirmed by more intense and/or additional $\{hkl\}$ reflections in the plan-view TEM diffraction patterns. During ion-induced grain growth, new crystallographic facets have moved into the Bragg scattering condition, generating the additional rings in the diffraction pattern and the increase in diffraction contrast in the bright field image. Qualitatively, this texture evolution appears to be more prominent in the FePt 25 at. % film. This film initially exhibited only a strong {111} reflection but diffracted several $\{hkl\}$ reflections with increasing dosage. This initially strong {111} preferred fiber texture is suspected to be a result of the larger film thickness (50 nm) of FePt 25 at. % as compared to that of FePt (25 nm). As a film grows, the initial competing textures are lost to a preferred low energy surface for all subsequently deposited atoms.[30] The irradiation induced loss of the strong {111} reflection in FePt 25 at. % to several $\{hkl\}$ reflections indicates a change in the texture of the film.

Once critical doses of 4.0 dpa for FePt and 2.2 dpa for FePt 25 at. % were achieved, the grains were no longer disconnected. The loss of disconnected regions between grains, referred to as fissure area in Fig. 5, indicates a mass flow over the substrate surface that was facilitated by the ion bombardment. Previous reports for dense metals grown at thinner film thicknesses ($t<5$ nm) resulted in a dewetting of the film from the substrate during irradiation.[31] With increasing dosage, the amount of disconnected grain boundary area coverage, or fissure area, decreased, indicating negligible dewetting of these thicker films during ion bombardment.

Since no ordered intermetallics were observed during ambient temperature irradiation, a subsequent postion irradiated annealing was performed. The grain growth activation energies, estimated from K of Eq. (1), were found from the slopes in Fig. 6. The temperature dependent mobility of K is written as[24]

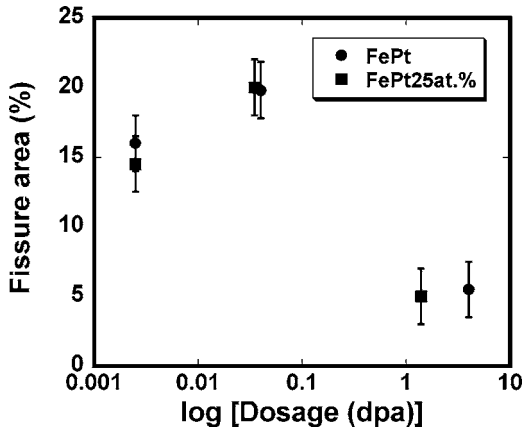

FIG. 5. Evolution of the fissure area between the grains with 500 keV Kr^+ irradiation.

$$K = K_o \exp(-Q/kT), \tag{2}$$

where K_o is a constant, Q is the activation energy, k is Boltzmann's constant, and T is the temperature. Q was found to be 0.83 ± 0.17 and 0.27 ± 0.01 eV for FePt and FePt 25 at. %, respectively. Though the datum is reasonably linear in Fig. 6, caution should be taken for the absolute value of these activation energy barriers. During annealing we have simultaneous grain growth and ordering, which occur at certain portions of the temperature regime. The nucleation and growth of new phases and stability of existing phases can contribute to several competing effects in the microstructure. Barmak *et al.*[32] have reported the activation energy for ordering in FePt to be ≈ 1.5 eV. From our results, we were not able to distinguish the effect of ordering to the observed grain growth activation energy.

For FePt, the onset of ordering, as indicated by the detection of superlattice reflections (001) and (110), was not evident until ≈ 550 °C, an ordering temperature which was slightly higher than the unirradiated FePt film. Additionally, the irradiated $L1_0$ phase was not able to achieve the lattice values equivalent to those of the unirradiated ordered film. The inability to lower the transformation temperature and/or recover the unirradiated lattice values would suggest that the defects created during irradiation have not been annihilated during ordering at these temperatures. Furthermore, the absence of a reduction in the ordering temperature suggests that the defects created in the cascade volume are relatively immobile. The use of light ion irradiation,[15–17] with its minimal defect disturbance of the lattice and freely migrating defects, is preferable for the promotion of this particular ordering transformation at lower temperatures.

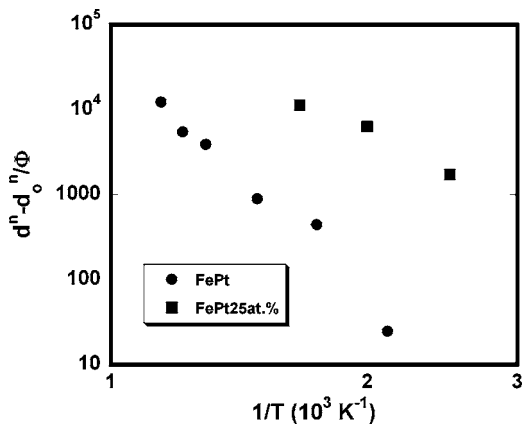

FIG. 6. Temperature dependence of $d^n - d_o^n/\Phi$ for FePt and FePt 25 at. %.

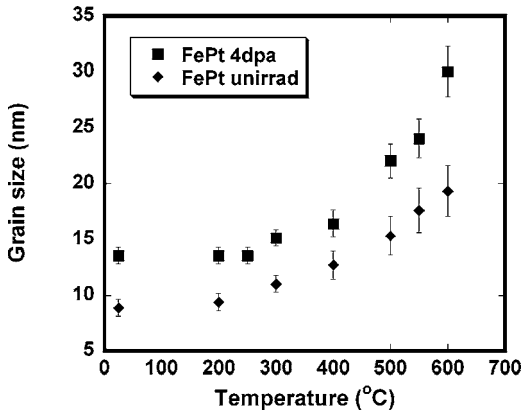

FIG. 7. Grain size as a function of temperature for both unirradiated and irradiated (4.0 dpa) FePt films.

At the onset of ordering, the unirradiated, disconnected granular microstructure exhibited the transition to a continuous film morphology with minimal fissure area between grains. Recently, Takahashi and Hono[20] suggested that the grain boundary created by the coalescence of grains enhances the kinetics of ordering. We were able to achieve a continuous granular film coverage prior to annealing for the irradiated FePt film. The creation of coalesced grain boundaries in our experiment did not facilitate the ordering reaction at a lower temperature. The heavy ion irradiation induced damage appears sufficient to hinder the ordering transformation. The irradiated film exhibited a similar rate in grain coarsening with temperature as compared to the unirradiated film (Fig. 7). The irradiation appears to have little to no effect on the postirradiation annealing for grain coarsening. From this observation, the defects formed in FePt by Kr^+ bombardment do not play a significant role in thermally activated, postirradiation grain coarsening in FePt.

The Kr^+ irradiated FePt 25 at. % film exhibited the onset of ordering at ≈ 300 °C. Unlike the FePt film, this phase transformation was lowered compared to the unirradiated film. Qualitatively, the $L1_2$ Fe_3Pt phase exhibits a slightly weaker bonding, as evidenced by its lower order-disorder temperature: Fe_3Pt is at ≈ 830 °C compared to FePt at ≈ 1300 °C.[33] The defect mobility created during Kr^+ irradiation for FePt 25 at. % was activated at a lower annealing temperature to promote the $L1_2$ phase transformation. This suggests that the nearest neighbor interactions to irradiation induced defects are not as tightly bound, as compared to the previous FePt specimen. Similar to irradiated $L1_0$ FePt, the irradiated $L1_2$ Fe_3Pt phase in the temperature range studied was not able to achieve its unirradiated $L1_2$ equilibrium lattice values. This indicates that a significant portion of defects are still present in the lattice even after ordering.

V. CONCLUSION

A series of FePt and FePt 25 at. % films was sputter deposited to thicknesses of 20–50 nm onto electron transpar-

ent amorphous silicon monoxide substrates. Each as-deposited film had the $A1$ phase and exhibited a disconnected granular structure. The films were irradiated with 500 keV Kr^+ to a dosage of 2–4 dpa. During ion irradiation both films exhibited a greater degree of diffraction contrast in the bright field image. No chemical ordering into either the $L1_0$ or $L1_2$ phases was observed during ambient temperature irradiation. Continual irradiation up to ≈3 dpa resulted in the evolution of the disconnected granular microstructure into a continuous granular film. Grain growth under the ion beam was most significant for the FePt alloy. The irradiated FePt ordered into the $L1_0$ phase at ≈550 °C, which was nearly equivalent to the controlled, unirradiated film. The FePt 25 at. % film ordered into $L1_2$ at a lower temperature compared to its controlled, unirradiated film. This work has shown a strong dependence on both the microstructure and ordering temperature as a function of irradiation dosage, composition, and ordered phase formation.

ACKNOWLEDGMENTS

Two of the authors (N.W.M. and G.B.T.) recognize the National Science Foundation Materials Research Science and Engineering Center (Grant No. DMR-0213985) for supporting this work. The IVEM/Accelerator facilities are supported by the U.S. Department of Energy, BES-Materials Sciences, under Contract No. W-31-109-Eng.-38.

[1]T. Kakeshita, T. Fukuda, M. Tsujiguchi, T. Saburi, R. Oshima, and S. Muto, Appl. Phys. Lett. **77**, 1502 (2000).
[2]H. Zeng, J. Li, J. P. Liu, Z. L. Wang, and S. Sun, Nature (London) **40**, 395 (2002).
[3]Y. Nakamura, K. Sumiyama, and M. Shiga, J. Magn. Magn. Mater. **12**, 127 (1979).
[4]S. Maat, A. J. Kellock, D. Weller, J. E. E. Baglin, and E. E. Fullerton, J. Magn. Magn. Mater. **265**, 1 (2003).
[5]D. A. Weller *et al.*, IEEE Trans. Magn. **36**, 10 (2000).
[6]J. Numazawa and H. Ohshima, J. Magn. Magn. Mater. **176**, 1 (1997).
[7]S. Kang, J. W. Harrell, and D. E. Nikles, Nano Lett. **2**, 1033 (2002).
[8]T. S. Vedantam, J. P. Liu, H. Zeng, and S. Sun, J. Appl. Phys. **93**, 7184 (2003).
[9]S. Sun, E. E. Fullerton, D. Weller, and C. B. Murray, IEEE Trans. Magn. **37**, 1239 (2001).
[10]T. J. Klemmer, C. Liu, N. Shukla, X. W. Wu, D. Weller, M. Tanase, D. E. Laughlin, and W. A. Soffa, J. Magn. Magn. Mater. **266**, 79 (2003).
[11]Y. K. Takahashi, T. Ohkubo, M. Ohnuma, and K. Hono, J. Appl. Phys. **93**, 7166 (2003).
[12]M. Miller and K. Albe, Phys. Rev. B **72**, 094203 (2005).
[13]R. V. Chepulskii, J. Velev, and W. H. Butler, J. Appl. Phys. **97**, 10J311 (2005).
[14]B. Yang, M. Asta, O. N. Mryasov, T. J. Klemmer, and R. W. Chantrell, Scr. Mater. **53**, 417 (2005).
[15]H. Bernas *et al.*, Phys. Rev. Lett. **91**, 077203 (2003).
[16]D. Ravelosona, C. Chappert, and V. Mathet, J. Appl. Phys. **87**, 5771 (2000).
[17]D. Ravelosona *et al.*, IEEE Trans. Magn. **37**, 1643 (2001).
[18]C.-H. Lai, C.-H. Yang, and C. C. Chiang, Appl. Phys. Lett. **83**, 4550 (2003).
[19]IMAGEJ, National Institute of Health, 1998.
[20]Y. K. Takahashi and K. Hono, Scr. Mater. **53**, 403 (2005).
[21]N. Karpe, J. Bottiger, N. G. Chechenin, and J. P. Krog, Mater. Sci. Eng., A **179/180**, 582 (1994).
[22]S. G. Mayr and R. S. Averback, Phys. Rev. B **68**, 075419 (2003).
[23]J. C. Liu, M. Nastasi, and J. W. Mayer, J. Appl. Phys. **62**, 423 (1987).
[24]J. C. Liu, J. Li, and J. W. Mayer, J. Appl. Phys. **67**, 2354 (1990).
[25]N. Nita, R. Schaeublin, and M. Victoria, J. Nucl. Mater. **329–333**, 953 (2004).
[26]J. S. Koehler and F. Seitz, Solid State Phys. **2**, 307 (1956).
[27]R. S. Averback and T. D. Rubia, Solid State Phys. **51**, 281 (1998).
[28]B. Rellinghaus, E. Mohn, L. Schultz, T. Gemming, M. Acet, A. Kowalik, and B. F. Kock, IEEE Trans. Magn. **42**(10), 3048–3051 (2006).
[29]W. Voegeli, K. Albe, and H. Hahn, Nucl. Instrum. Methods Phys. Res. B **202**, 230 (2003).
[30]C. V. Thompson, Annu. Rev. Mater. Sci. **30**, 159 (2000).
[31]X. Hu, D. G. Cahill, R. S. Averback, and R. C. Birtcher, J. Appl. Phys. **93**, 165 (2003).
[32]K. Barmak, J. Kim, D. C. Berry, W. N. Hanani, K. Wierman, E. B. Svedberg, and J. K. Howard, J. Appl. Phys. **97**, 024902 (2005).
[33]*Binary Alloy Phase Diagrams*, edited by T. B. Massalski (ASM International, Metals Park, OH, 1990), p. 1752.